

Spectral-luminescence properties of ZrO_2 – Sc_2O_3 – Tb_2O_3 crystals

© S.Kh. Batygov¹, M.A. Borik¹, A.V. Kulebyakin¹, N.A. Larina², E.E. Lomonova¹, V.A. Myzina¹, P.A. Ryabochkina^{2¶}, N.V. Sidorova², A.D. Taratynova², N.Yu. Tabachkova^{1,3}

¹ Prokhorov Institute of General Physics, Russian Academy of Sciences, Moscow, Russia

² Ogarev Mordovian State University, 430005 Saransk, Russia

³ National University of Science and Technology MISiS, Moscow, Russia

¶ e-mail: ryabochkina@freemail.mrsu.ru

Received June 28, 2021

Revised June 28, 2021

Accepted September 08, 2021

Crystals of the concentration series ZrO_2 –(8–10) mol.% Sc_2O_3 –(1–2) mol.% Tb_2O_3 were grown by the method of directional crystallization of the melt from a cold container. Analysis of the spectral-luminescence characteristics of these crystals after growth and after annealing processing in a vacuum revealed the presence of both Tb^{3+} and Tb^{4+} ions in them. In crystals ZrO_2 –(8–10) mol.% Sc_2O_3 –(1–2) mol.% Tb_2O_3 , the presence of a process of non-radiative energy transfer from Tb^{4+} ions to Tb^{3+} ions was revealed.

Keywords: solid solutions of zirconium dioxide, luminescence, terbium ions.

DOI: 10.21883/EOS.2022.01.52991.20-21

Introduction

Materials doped with terbium ions attract considerable interest from researchers. This is due to a wide range of their applications in the production of LEDs, X-ray and cathodoluminescent screens, scintillators, as well as the potential use of these materials for the development of volume optical memory, high-energy radiation dosimetry, medical diagnostics and bioimaging [1–7].

Many practical applications are due to the luminescence presence in trivalent terbium ions in the visible range of the spectrum due to optical transitions $^5D_4 \rightarrow ^7F_J$ ($J = 2, 3, 4, 5, 6$). However, depending on the chemical nature of the matrix, the conditions of its synthesis and processing the terbium can present in it with oxidation states of both 3+ and 4+. The presence of both Tb^{3+} and Tb^{4+} ions in the composition of the compound has a significant effect on the luminescence efficiency of Tb^{3+} ions. Tb^{4+} ions do not contribute to radiation in the visible region, and in some cases, due to the presence of absorption bands in the visible region of spectra of Tb^{4+} ions, they can contribute to luminescence quenching of Tb^{3+} ions [8,9]. Consequently, the oxidation of Tb^{3+} ions is one of the problems for materials whose application is based on their luminescent properties.

Crystals based on zirconium dioxide are a promising material serving as a matrix for rare earth (RE) elements with luminescence properties. Thanks to their thermal and chemical stability and high refractive index, single crystals and polycrystals based on ZrO_2 doped with RE ions are of interest for various practical applications (optical products, material for electrolytic membranes of solid oxide fuel cells, biomedical materials, phosphors, etc.) [10–14]. Currently, there are numerous studies of compounds based

on zirconium dioxide compounds activated by various RE elements: Eu^{3+} [15–18], Er^{3+} [19–22], Dy^{3+} [23–25], Ce^{3+} [26,27] etc.

Studies of the spectroscopic characteristics of films, nanosized particles and fibers based on ZrO_2 doped with terbium ions are the subject of papers [28–31]. At the same time, studies on the spectral-luminescence characteristics of terbium ions in single crystals based on zirconium dioxide have not been carried out by now. Accordingly, the purpose of this paper was to study the spectral-luminescence properties of ZrO_2 – Sc_2O_3 – Tb_2O_3 crystals immediately after growth, as well as after annealing of these crystals in a reducing atmosphere (vacuum).

Characteristics of objects and research methods

For research, ZrO_2 – Sc_2O_3 – Tb_2O_3 crystals were grown. Crystals were grown by direct high-frequency heating in a cold crucible on a „Kristall-407“ unit with the crucible diameter of 130 mm and the crucible lowering rate of 10 mm/h. The compositions and the corresponding designations of crystals used further in the work are given in the Table.

After growth the crystals of compositions 1–5 were subjected to heat treatment in reducing atmosphere (vacuum) at a temperature of 1600°C for 4 h.

The phase composition of the crystals was studied by Raman spectroscopy using a Renishaw InVia confocal microscope-spectrograph ($\lambda_{ex} = 532$ nm, $\lambda_{ex} = 632$ nm).

Absorption spectra were recorded on a Perkin Elmer Lambda 950 spectrophotometer.

Chemical composition and symbols of crystals

N ^o	Composition	Designation
1	91 mol.% ZrO_2 –8 mol.% Sc_2O_3 –1 mol.% Tb_2O_3	8Sc1TbSZ
2	90 mol.% ZrO_2 –8 mol.% Sc_2O_3 –2 mol.% Tb_2O_3	8Sc2TbSZ
3	90 mol.% ZrO_2 –9 mol.% Sc_2O_3 –1 mol.% Tb_2O_3	9Sc1TbSZ
4	89 mol.% ZrO_2 –9 mol.% Sc_2O_3 –2 mol.% Tb_2O_3	9Sc2TbSZ
5	89 mol.% ZrO_2 –10 mol.% Sc_2O_3 –1 mol.% Tb_2O_3	10Sc1TbSZ

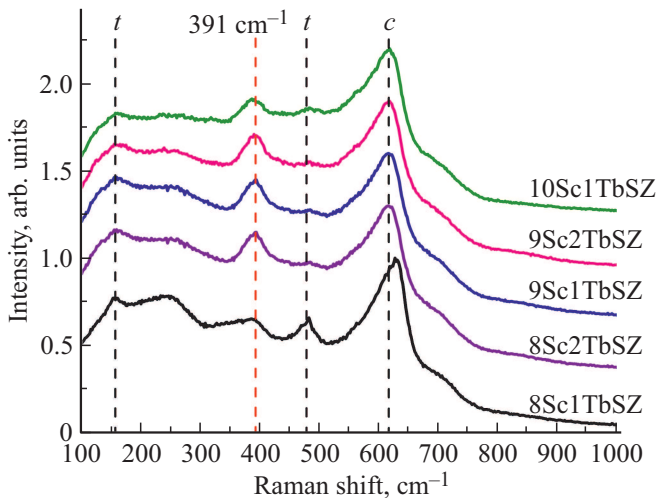


Figure 1. Raman spectra of 8Sc1TbSZ, 8Sc2TbSZ, 9Sc1TbSZ, 9Sc2TbSZ, 10Sc1TbSZ crystals after growth ($\lambda_{ex} = 532$ nm, $T = 300$ K).

The luminescence spectra were recorded using a Horiba FHR 1000 monochromator under laser excitation $\lambda_{ex} = 351$ nm.

The excitation spectra were recorded on an RF-5301PC spectrofluorimeter (Shimadzu) using a xenon lamp as an excitation source.

Research results

Figure 1 shows the Raman spectra of crystals with compositions 1–5 after growth, recorded under excitation by laser radiation with a wavelength $\lambda_{ex} = 532$ nm.

The presence in Raman spectra of a characteristic line with a maximum of ~ 617 cm^{-1} [32–34] indicates that all crystals after growth predominantly have a cubic structure. Also, in the Raman spectra of samples 8Sc1TbSZ, 8Sc2TbSZ, 9Sc1TbSZ the low-intensity lines ~ 150 cm^{-1} and 478 cm^{-1} , inherent to the tetragonal t phase [35–37] and a band with a maximum of 391 cm^{-1} , which was not previously detected in the characteristic Raman spectra of compounds based on zirconium dioxide, were identified. To establish the nature of this band occurrence Raman spectra were recorded upon excitation by laser radiation with a wavelength of $\lambda_{ex} = 633$ nm (Fig. 2). As can be seen, as the excitation wavelength changes, the

Raman spectra contain bands corresponding to the cubic (c) and tetragonal (t) phases, while the band with maximum of 391 cm^{-1} is absent. Therefore, we can conclude that this band occurrence is due to the length choice of the excitation wave and is not related to the structural features of the crystals under study.

For more detailed study of the presence of Tb^{3+}/Tb^{4+} ions in $ZrO_2-Sc_2O_3-Tb_2O_3$ crystals, as well as to establish possible reasons for the line occurrence in the Raman spectra in 391 cm^{-1} region the absorption spectra of terbium ions were recorded in the range of $200-3300$ nm (Fig. 3). The assumption of the presence in $ZrO_2-Sc_2O_3-Tb_2O_3$ crystals grown in air of both Tb^{3+} and Tb^{4+} ions is due to introduction of Sc_2O_3 and Tb_2O_3 oxides in the solid solutions based on zirconium dioxide is accompanied by the formation of anion vacancies (V_O), which are formed due to different valences of Zr^{4+} and R^{3+} ($R - Sc, Tb$).

Absorption spectra of $ZrO_2-Sc_2O_3-Tb_2O_3$ crystals after growth (Fig. 3) is represented by a wide band in the range of $340-580$ nm, due to transition of charge $O^{2-} \rightarrow Tb^{4+}$, as well as by a number of lines in the IR region corresponding to intraconfigurational $4f-4f$ optical transitions from the ground state 7F_6 to excited multiplets ${}^7F_{0,1,2}$, ${}^7F_6 \rightarrow {}^7F_3$, ${}^7F_6 \rightarrow {}^7F_4$ of Tb^{3+} ions.

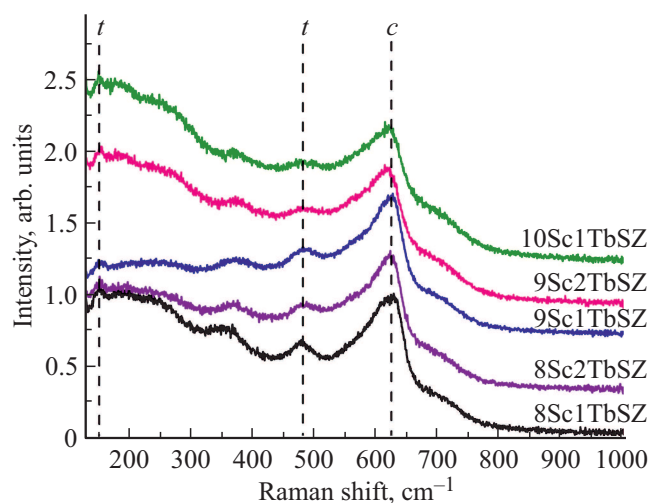


Figure 2. Raman spectra of 8Sc1TbSZ, 8Sc2TbSZ, 9Sc1TbSZ, 9Sc2TbSZ, 10Sc1TbSZ crystals after growth ($\lambda_{ex} = 633$ nm, $T = 300$ K).

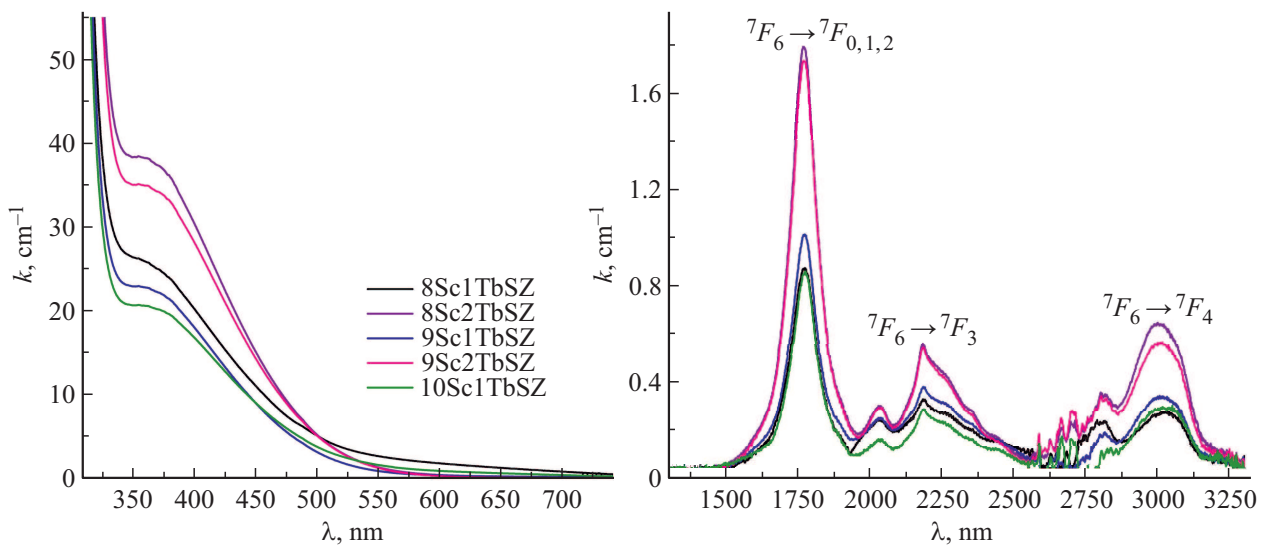


Figure 3. Absorption spectra of Tb^{3+}/Tb^{4+} ions in 8Sc1TbSZ, 8Sc2TbSZ, 9Sc1TbSZ, 9Sc2TbSZ, 10Sc1TbSZ crystals after growth ($T = 300$ K).

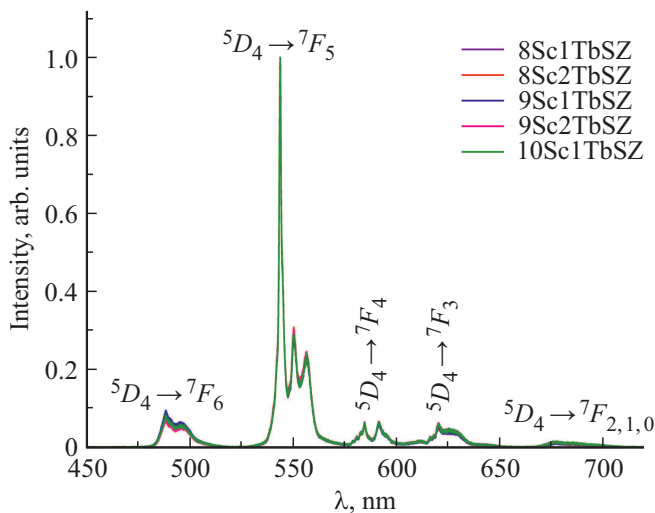


Figure 4. Luminescence spectra of Tb^{3+} ions of 8Sc1TbSZ, 8Sc2TbSZ, 9Sc1TbSZ, 9Sc2TbSZ, 10Sc1TbSZ crystals after growth ($\lambda_{ex} = 351$ nm).

It can be seen from the absorption spectra shown in Fig. 3 that the radiation wavelength used to excite the Raman spectra, and equal to 532 nm, falls on the edge of the absorption band of Tb^{4+} ions. Since Tb^{4+} ions have no radiative transitions in the visible spectral range, the 391 cm^{-1} (543 nm) line cannot be due to the luminescence of Tb^{4+} ions. Along with this, the most intense luminescence bands of Tb^{3+} ions are present in the green region of the spectrum. This is confirmed by the luminescence spectra of crystals with compositions 1–5, recorded upon excitation by radiation with wavelength of 351 nm to the level 5D_3 of Tb^{3+} ions (Fig. 4). The most intensive lines in the spectrum with maxima ~ 489 , ~ 543 , ~ 584 , and ~ 620 nm refer

to optical transitions $^5D_4 \rightarrow ^7F_6$, $^5D_4 \rightarrow ^7F_5$, $^5D_4 \rightarrow ^7F_4$ and $^5D_4 \rightarrow ^7F_3$ of Tb^{3+} ions, respectively. A change in the concentration of Sc_2O_3 and Tb_2O_3 oxides in the crystals under study does not affect the ratio of the line intensities in the luminescence spectra.

Comparison of the Raman spectra and luminescence spectra of $ZrO_2-Sc_2O_3-Tb_2O_3$ crystals revealed that the position of the line with maximum of 391 cm^{-1} observed in the Raman spectra coincides with the maximum in the luminescence spectrum corresponding to the most intensive transition $^5D_4 \rightarrow ^7F_5$ of Tb^{3+} ions (Fig. 5, a).

The mechanism of energy transfer from Tb^{4+} ions to Tb^{3+} ions, which causes the luminescence of trivalent terbium ions upon excitation $\lambda_{ex} = 532$ nm, is shown in Fig. 5, b) and is as follows. Tb^{4+} ions, due to the absorption of laser radiation $\lambda_{ex} = 532$ nm, pass from the ground state to the excited state. As a result of the nonradiative energy transfer from Tb^{4+} ions to Tb^{3+} ions, the former are in the ground state, and Tb^{3+} ions from the ground state 3F_4 go to level 5D_4 . Luminescence is observed from 5D_4 level of Tb^{3+} ions due to $^5D_4 \rightarrow ^7F_5$ transition of Tb^{3+} ions with maximum of 543 nm, which corresponds to 391 cm^{-1} line in the Raman spectra.

For further study of the degree of oxidation of terbium ions in $ZrO_2-Sc_2O_3-Tb_2O_3$ crystals, the crystals were annealed at a temperature of 1600°C in reducing atmosphere (vacuum) for 4 h.

From Fig. 6 it is evident that after annealing two regions, i.e. transparent (1) and dark opaque in the visible spectral range (2), formed in the crystals.

The formation of a dark region is apparently associated with the formation of a color center, the presence of a transparent region is due to change in the valence $Tb^{4+} \rightarrow Tb^{3+}$. This is confirmed by the absorption spectra of 8Sc1TbSZ, 8Sc2TbSZ, 9Sc1TbSZ, 9Sc2TbSZ, and 10Sc1TbSZ crystals

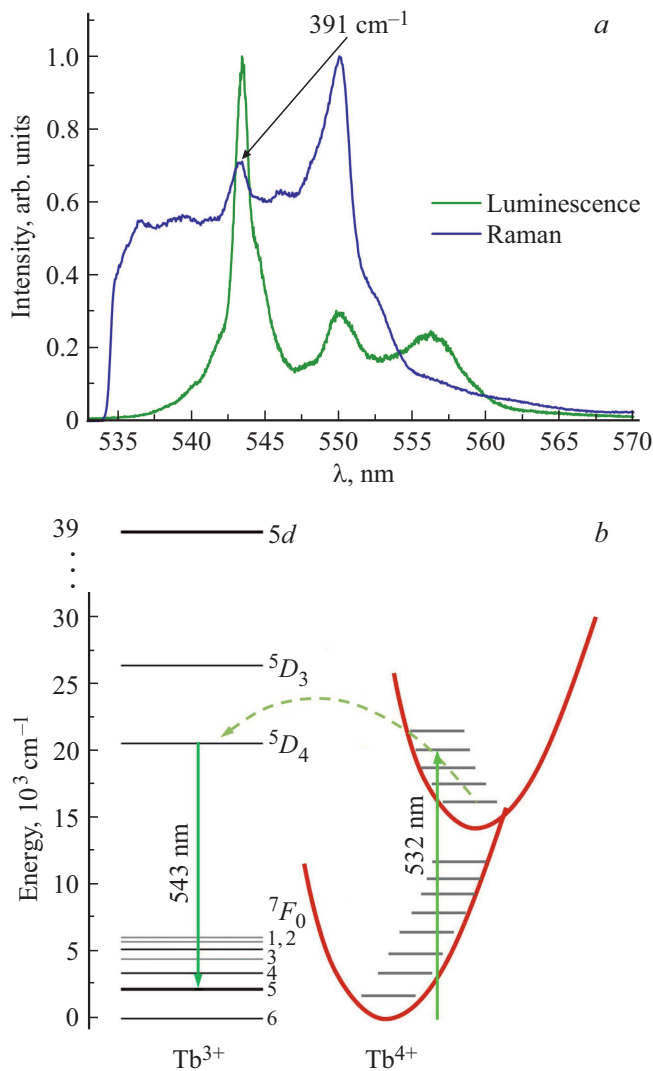


Figure 5. *a* — Raman and luminescence spectra for ${}^5D_4 \rightarrow {}^7F_3$ transition of Tb^{3+} ions in 9Sc2TbSZ crystal, *b* — scheme of energy transfer between Tb^{4+} and Tb^{3+} ions.

recorded after vacuum annealing (Fig. 7). The appearance in the absorption spectrum of a wide band in the region of 340–800 nm, which is absent in the spectrum of crystals after growth, is associated with the presence of color centers (Fig. 7).

Figure 8 shows the excitation spectra of $ZrO_2-Sc_2O_3-Tb_2O_3$ crystals before and after vacuum annealing ($\lambda_{em} = 543$ nm). In the excitation spectra of the crystals shown in Fig. 8, *a–d*, a wide asymmetric band is observed in the range from 220 to 350 nm with a maximum of ~ 290 nm, and also lines with maxima ~ 380 and ~ 488 nm, due to ${}^7F_6 \rightarrow {}^5D_3$, ${}^7F_6 \rightarrow {}^5D_4$ transitions of Tb^{3+} ions, respectively.

To reveal the reason for the formation of the complex contour of 220–350 nm band, the comparative analysis of the excitation spectra of 8Sc2TbSZ, 9Sc1TbSZ, 9Sc2TbSZ, and 10Sc1TbSZ crystals after growth and after vacuum annealing (Fig. 8) was carried out, it made possible

to reveal the following regularities. In the excitation spectra recorded for region of the crystal *I*, this band becomes more asymmetric, and its maximum shifts to longer wavelengths ~ 319 nm as compared to the position of the similar line in the crystal spectrum after growth (~ 289 nm). The transformation of the excitation spectra of crystals after heat treatment in vacuum can be explained as follows. The line with a maximum ~ 319 nm is due to $4f^8 \rightarrow 4f^75d^1$ transitions of Tb^{3+} , this is confirmed by the relative intensity increasing of this line for the corresponding regions of crystals after vacuum annealing, due to the change in valence $Tb^{4+} \rightarrow Tb^{3+}$. This fact confirms the relative increase in the lines for the ${}^5D_3 \rightarrow {}^7F_6$, ${}^5D_4 \rightarrow {}^7F_6$ transitions of Tb^{3+} ions in the excitation spectra of crystals after vacuum annealing in comparison with similar lines in the excitation spectra of post-growth crystals.

Another proof of the relative increasing of the line ~ 319 nm in the excitation spectra for region 1 of the crystals under study as the result of the change in valence $Tb^{4+} \rightarrow Tb^{3+}$ is the increasing of the absorption coefficient

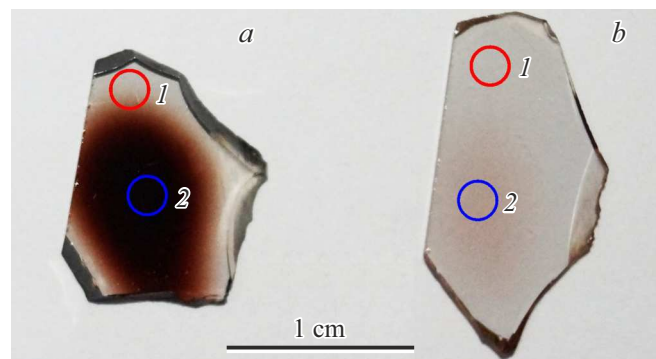


Figure 6. Photo of plates cut from 9Sc2TbSZ (*a*), 10Sc1TbSZ (*b*) crystals after vacuum annealing at temperature of $= 1600^\circ C$, $t = 4$ h.

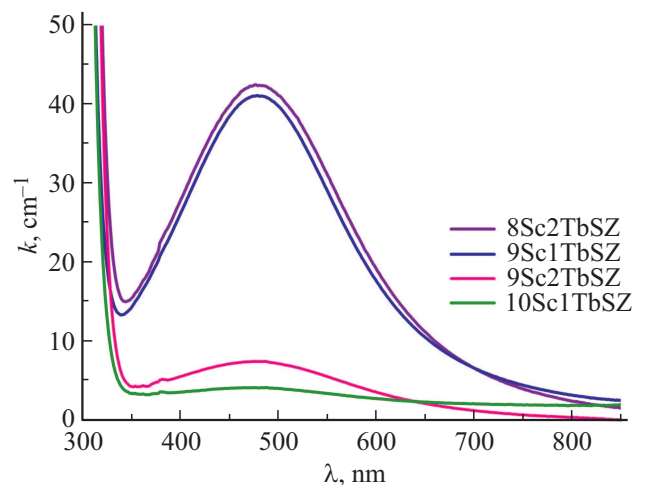


Figure 7. Absorption spectra of 8Sc2TbSZ, 9Sc1TbSZ, 9Sc2TbSZ, 10Sc1TbSZ crystals after vacuum annealing at $1600^\circ C$, $t = 4$ h ($T = 300$ K).

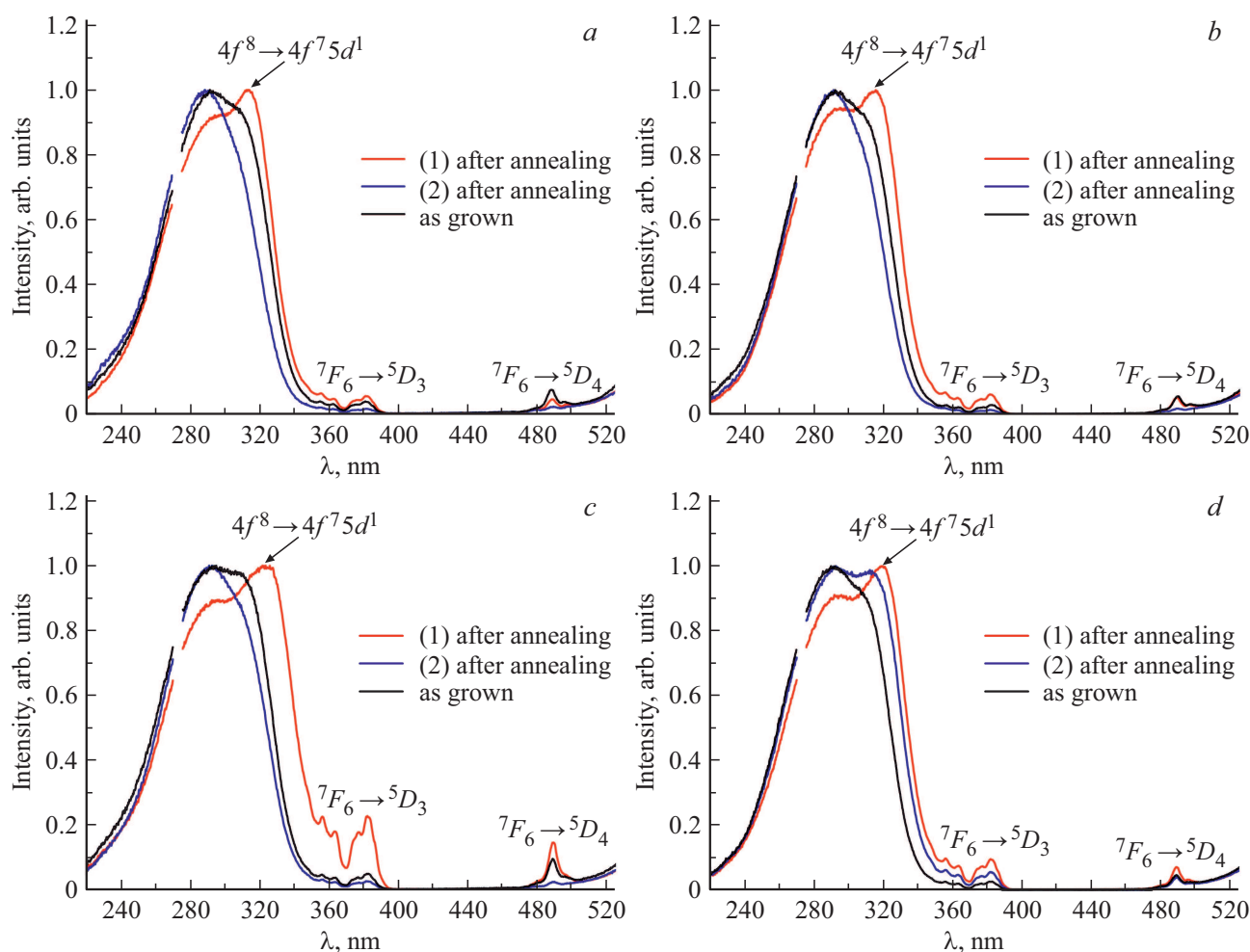


Figure 8. Excitation spectra of 8Sc2TbSZ (a), 9Sc1TbSZ (b), 9Sc2TbSZ (c), 10Sc1TbSZ (d) crystals after vacuum annealing at 1600°C, $t = 4$ h ($\lambda_{\text{em}} = 543$ nm, $T = 300$ K).

of Tb^{3+} ions for ${}^7F_6 \rightarrow {}^7F_{0,1,2}$, ${}^7F_6 \rightarrow {}^7F_3$, ${}^7F_6 \rightarrow {}^7F_4$ transitions in the absorption spectra (Fig. 9) and the line absence in the range of 340–580 nm, associated with the charge transfer band of Tb^{4+} ions.

In the excitation spectra for region 2 of crystals after recovery annealing, the following can be noted. The band in the region of 220–350 nm in the excitation spectra of crystals after annealing becomes more symmetric, the position of its maximum is retained with respect to the spectra of crystals after growth (except for 10Sc1TbSZ sample, where the area of this region is minimum). Apparently, the band with maximum ~ 289 nm is due to the ionization transition of the electron from the Tb^{3+} ion in the ground state to the conduction band. This mechanism was proposed by the authors [38] when determining the nature of the line with maximum of ~ 282 nm observed by them in the excitation spectra of $\text{Y}_2\text{O}_3\text{:Tb}$ crystals. Also, due to the presence of oxygen vacancies in solid solutions based on zirconium dioxide, this band can be determined by $\text{Tb}^{3+} - \text{V}_\text{o}^{2+}$ transition, i.e. electron transition from Tb^{3+} ions to oxygen vacancy.

Conclusion

Thus, in this paper, crystals of the concentration series were synthesized, they were subsequently subjected to heat treatment in vacuum at 1600°C for 4 h.

Study of $\text{ZrO}_2 - (8-10) \text{ mol.}\% \text{Sc}_2\text{O}_3 - (1-2) \text{ mol.}\% \text{Tb}_2\text{O}_3$ crystals by Raman spectroscopy identified the presence of cubic phase in them. Also, in the Raman spectra of 8Sc1TbSZ, 8Sc2TbSZ, 9Sc1TbSZ crystals, low-intensity lines ~ 150 and 470 cm^{-1} inherent to the tetragonal t phase were found.

Results of studies of the spectral-luminescent properties of $\text{ZrO}_2 - (8-10) \text{ mol.}\% \text{Sc}_2\text{O}_3 - (1-2) \text{ mol.}\% \text{Tb}_2\text{O}_3$ crystals indicate the presence of both Tb^{3+} ions and Tb^{4+} ions. Upon excitation into charge transfer band $\text{O}^{2-} \rightarrow \text{Tb}^{4+}$, a process of nonradiative energy transfer from Tb^{4+} ions to Tb^{3+} ions was observed.

The vacuum annealing of $\text{ZrO}_2 - (8-10) \text{ mol.}\% \text{Sc}_2\text{O}_3 - (1-2) \text{ mol.}\% \text{Tb}_2\text{O}_3$ crystals at 1600°C for $t = 4$ h leads to the color centers occurrence in them and the terbium ions transition from the tetravalent state to the trivalent state.

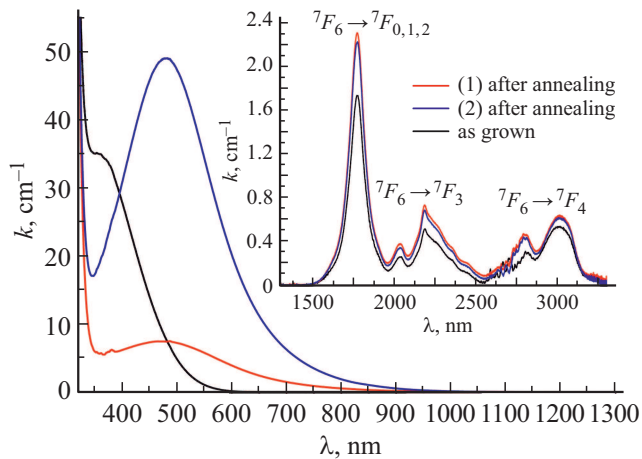


Figure 9. Absorption spectra recorded for (1) and (2) regions of 9Sc2TbSZ crystals after vacuum annealing at 1600°C, ($T = 300$ K).

Funding

This study was financially supported by the grant of Russian Science Foundation № 19-72-10113. Structure study was performed using equipment of „Materials Science and Metallurgy“ Common Use Center with financial support of the Russian Federation presented by the Ministry of Education and Science (№ 075-15-2021-696).

Conflict of interest

The authors declare that they have no conflict of interest.

References

- [1] B. Dhabekar, S.N. Menon, E. Alagu Raja, A.K. Bakshi, A.K. Singh, M.P. Chougaoonkar, Y.S. Mayya. *Beam Interactions with Materials and Atoms*, **269**(16), 1844 (2011). DOI: 10.1016/j.nimb.2011.05.001
- [2] Guifang Li, Quanxi Cao, Zhimin Li, Yunxia Huang, Yunge Wei, Junyan Shi. *J. All. Comp.*, **485**(1–2), 561 (2009). DOI: 10.1016/j.jallcom.2009.06.026
- [3] C.C. Kang, R.S. Liu. *J. Lumin.*, **122**, 574 (2007). DOI: 10.1016/j.jlumin.2006.01.228
- [4] P.W. Metz, D.T. Marzahl, A. Majid, C. Kränkel, G. Huber. *Laser Photon. Rev.*, **10**, 35 (2016). DOI: 10.1002/lpor.201500274
- [5] Bin Lu, Ji-Guang Li, Xudong Sun, Yoshio Sakka. *J. Am. Ceram. Soc.*, **98**(12), 3877 (2015). DOI: 10.1111/jace.13834
- [6] E. Cavalli, E.A. Volkova. *Journal of Solid State Chemistry*, **301**, 122306 (2021). DOI: 10.1016/j.jssc.2021.122306
- [7] K. Okamoto, T. Ebina, N. Fujii, K. Konishi, Yu Sato, T. Kashima, R. Nakano, H. Hioki, H. Takeuchi, J. Yumoto, M. Matsuzaki, Y. Ikegaya. *Sci. Adv.*, **7**(7), eabd2529 (2021). DOI: 10.1126/sciadv.abd2529
- [8] R.K. Verma, K. Kumar, S.B. Rai. *Solid State Sci.*, **12**(7), 1146 (2010). DOI: 10.1016/j.solidstatesciences.2010.04.004
- [9] H.-Y. He. *Micro and Nanosystems*, **8**(2), 114 (2016). DOI: 10.2174/1876402909666170126122221
- [10] B. Sathyaseelan, E. Manikandan, I. Baskaran, K. Senthilnathan, K. Sivakumar, M.K. Moodley, R. Ladhumananandasivam, M. Maaza. *J. All. Comp.*, **694**, 556 (2017). DOI: 10.1016/j.jallcom.2016.10.002
- [11] P. Vařák, J. Mrázek, W. Blanc, J. Aubrecht, M. Kamrádek, O. Podrazký, P. Honzátko. In: *Micro-structured and Specialty Optical Fibres VII*, ed. by K. Kalli, A. Mendez, P. Peterka. (Proceedings of SPIE, Bellingham, Washington USA, 2021), vol. 11773, p. 1177317. DOI: 10.1117/12.2589127
- [12] P.A. Ryabochkina, A.N. Chabushkin, A.A. Lyapin, E.E. Lomonova, N.G. Zakharov, K.V. Vorontsov. *Laser Phys. Lett.*, **14**(5), 055807 (2017). DOI: 10.1088/1612-202X/aa69a5
- [13] C. Petit, L. Montanaro, P. Palmero. *International Journal of Applied Ceramic Technology*, **15**(4), 820 (2018). DOI: 10.1111/ijac.12878
- [14] Tae-Yun Kang, Ji-Young Seo, Jeong-Hyun Ryu, Kwang-Mahn Kim, Jae-Sung Kwon. *Journal of Biomedical Materials Research*, **109**(7), 1196 (2021). DOI: 10.1002/jbm.a.37113
- [15] K. Smits, L. Grigorjeva, D. Millers, A. Sarakovskis, A. Opalinska, J.D. Fidelus, W. Lojkowski. *Optical Materials*, **32**(8), 827 (2010). DOI: 10.1016/j.optmat.2010.03.002
- [16] M.R.N. Soares, C. Nico, D. Oliveira, M. Peres, L. Rino, A.J.S. Fernandes, T. Monteiro, F.M. Costa. *Materials Science and Engineering: B*, **177**(10), 712 (2012). DOI: 10.1016/j.mseb.2011.10.010
- [17] S.D. Meetei, S.D. Singh. *J. Lumin.*, **147**, 328 (2014). DOI: 10.1016/j.jlumin.2013.11.064
- [18] M.A. Borik, T.V. Volkova, I.E. Kuritsyna, E.E. Lomonova, V.A. Myzina, P.A. Ryabochkina, N.Yu. Tabachkova. *J. All. Comp.*, **770**, 320 (2019). DOI: 10.1016/j.jallcom.2018.08.117
- [19] E. De La Rosa-Cruz, L.A. Díaz-Torres, R.A. Rodríguez-Rojas, M.A. Meneses-Nava, O. Barbosa-García, P. Salas. *Appl. Phys. Lett.*, **83**, 4903 (2003). DOI: 10.1063/1.1632020
- [20] P.A. Ryabochkina, N.V. Sidorova, S.N. Ushakov, E.E. Lomonova. *Quant. Electron.*, **44**(2), 135 (2014). DOI: 10.1070/QE2014v044n02ABEH015276
- [21] M.R.N. Soares, T. Holz, F. Oliveira, F.M. Costa, T. Monteiro. *RSC Adv.*, **5**(26), 20138 (2015). DOI: 10.1039/C5RA00189G
- [22] S. Stojadinovic, N. Tadic, R. Vasilic. *Mater. Lett.*, **219**, 251 (2018). DOI: 10.1016/j.matlet.2018.02.126
- [23] K. Srigurunathan, R. Meenambal, A. Guleria, D. Kumar, J.M. da F. Ferreira, S. Kannan. *ACS Biomater. Sci. Eng.*, **5**, 1725 (2019). DOI: 10.1021/acsbomaterials.8b01570
- [24] A. Ćirić, S. Stojadinović. *J. All. Comp.*, **832**, 154907 (2020). DOI: 10.1016/j.jallcom.2020.154907
- [25] D. Prakashbabu, H.B. Ramalingam, R. Hari Krishna, B.M. Nagabhushana, C. Shivakumara, K. Munirathnam, S. Ponkumar. *J. Lumin.*, **192**, 496 (2017). DOI: 10.1016/j.jlumin.2017.07.015
- [26] C. Tiseanu, V. Parvulescu, D. Avram, B. Cojocar, M. Boutonnet, M. Sanchez-dominguez. *Phys. Chem. Chem. Phys.*, **16**, 703 (2014). DOI: 10.1039/c3cp52893f
- [27] I. Ahemen, F.B. Dejene. *J. Mater. Sci.: Mater. Electron.*, **29**, 2140 (2018). DOI: 10.1007/s10854-017-8126-5
- [28] X. Qu, H.K. Yang, B.K. Moon, B.C. Choi, J.H. Jeong. *Jpn. J. Appl. Phys.*, **50**, 01AK06 (2011). DOI: 10.1143/JJAP.50.01AK06
- [29] V.R. Panse, N.S. Kokode, S.J. Dhoble. *Optik*, **126**, 4782 (2015). DOI: 10.1016/j.ijleo.2015.07.062

- [30] Fu Ning, Wang Xixin, Guo Limin, Zhao Jianling, Zhang Xinghua, Lin Jing, Gong Liyuan, Wang Mingli, Yang Yang. *J. Mater. Sci: Mater. Electron.*, **28**, 7253 (2017). DOI: 10.1007/s10854-017-6407-7
- [31] Yizhu Xie, Ziwei Ma, Lixin Liu, Yuroug Su, Haiting Zhao, Yanxia Liu, Zhenxing Zhang, Huigao Duan, Jian Li, Erqing Xie. *Appl. Phys. Lett.*, **97**, 141916 (2010). DOI: 10.1063/1.3496471
- [32] A. Feinberg, C.H. Perr. *J. Phys. Chem. Solids*, **42** (2), 513 (1981). DOI: 10.1016/0022-3697(81)90032-9
- [33] M. Ishigame, E. Yoshid. *Solid State Ionics*, **23** (2), 211 (1987). DOI: 10.1016/0167-2738(87)90053-1
- [34] M. Yashima, K. Ohtake, M. Kakihana, H. Arashi, M. Yoshimura. *J. Phys. Chem. Solids*, **57** (1), 17 (1996). DOI: 10.1016/0022-3697(95)00085-2
- [35] V.I. Aleksandrov, Yu.K. Voron'ko, B.V. Ignat'ev, E.E. Lomonova, V.V. Osiko, A.A. Sobol. *Sov. Phys. Sol. State*, **20** (2), 305 (1978).
- [36] C.H. Perry, D-W. Liu, L.R.P. Ingel. *J. Am. Ceram. Soc.*, **68** (8), 184 (1985). DOI: 10.1111/j.1151-2916.1985.tb10176.x
- [37] Y. Hemberger, N. Wichtner, C. Berthold, K.G. Nickel. *International Journal of Applied Ceramic Technology*, **13** (1), 116 (2016). DOI: 10.1111/ijac.12434
- [38] M. Behrendt, S. Mahlik, K. Szczodrowski, B. Kuklińska, M. Grinberg. *Phys. Chem. Chem. Phys.*, **18**, 22266 (2016). DOI: 10.1039/C6CP03075K